IEEE Access
Multidisciplinary | Rapid Review | Open Access Journal

Received December 4, 2019, accepted December 25, 2019, date of publication December 30, 2019, date of current version January 8, 2020.

Digital Object Identifier 10.1109/ACCESS.2019.2963102

Multi-Mode Switching Control of the EPS With Hybrid Power Supply

BIN TANG[1], YINGQIU HUANG[2], DI ZHANG[2], AND HAOBIN JIANG[2]
[1]Automotive Engineering Research Institute, Jiangsu University, Zhenjiang 212013, China
[2]School of Automotive and Traffic Engineering, Jiangsu University, Zhenjiang 212013, China

Corresponding author: Bin Tang (tangbin@ujs.edu.cn)

This work was supported in part by the National Natural Science Foundation of China under Grant 51605199, in part by the Natural Science Foundation of Jiangsu Province under Grant BK20160527, in part by the Six Talent Peaks Project of Jiangsu Province under Grant 2019-GDZB-084, and in part by the Special Fund for the Transformation of Scientific and Technological Achievements in Taizhou under Grant SCG201904.

ABSTRACT Electric power steering system (EPS) with traditional power supply can't provide enough power for heavy-duty vehicle to turn at low speed. To solve the problem, a novel EPS with hybrid power supply was constructed. In this paper, firstly, mathematical model of the EPS with hybrid power supply was established including model of hybrid power supply system and basic model of EPS. Then the power mode recognition was obtained according to the certain threshold of steering resistance torque, state of charge (SOC) of super-capacitor and output voltage of the vehicle power supply, and the corresponding finite automaton model was built. The EPS system with hybrid power supply was regarded as a hybrid system due to continuous event in a single mode and discrete event during mode switching process, thus the multi-mode switching control strategy was proposed. Taken the different characteristics of hybrid power supply in different power modes into account, the corresponding local controllers were designed which were consisted of fuzzy-PID controller, active disturbance rejection controller (ADRC) and sliding mode controller. Besides, the fuzzy supervisory controller was also designed to ensure the stability of the hybrid system during mode switching process. The simulation results show that the local controllers can achieve fast and accurate track of target current in each power mode, and the fuzzy supervisor can effectively ensure the stability of the switching process, which demonstrates the feasibility of the control strategy.

INDEX TERMS Hybrid power supply system, EPS, hybrid system, multi-mode switching, fuzzy supervisor controller.

I. INTRODUCTION

Recently, the HPS system is widely used in heavy-duty vehicles for its advantage of high steering assist effort [1]. However, the HPS system has some disadvantages of poor steering road feeling and high energy consumption [2], [3]. In order to solve the problems of HPS, some scholars have carried out some relevant researches. Xia *et al.* studied an electronically controlled hydraulic power steering system which can realize the variable assist characteristics and improve the high-speed steering road feeling [4]. Tang *et al.* applied an electromagnetic slip coupling to hydraulic power steering, which shows that the energy consumption decreases greatly compared with that of HPS [5]. The solutions mentioned above is proposed to adjust either hydraulic flow or pressure of HPS, thus the problems of HPS cannot be fundamentally solved.

The electric power steering (EPS) system widely used in passenger cars [6] has variable assist characteristics and can provide steering assist effort as required, which obviously improves the steering road feeling and greatly reduce the consumption of steering system [7], [8]. However, the EPS with traditional power supply cannot provide enough power for heavy-duty vehicles to turn at low speed, which limits the application of EPS in heavy-duty vehicles [9].

The super-capacitor, as a new type of energy storage device, has been widely applied in many energy sources recently because of its unique characteristics of large discharging current, fast charging rate and long cycle life [10], [11], which just compensates the shortcomings of traditional power supply. Therefore, the hybrid power supply

The associate editor coordinating the review of this manuscript and approving it for publication was Xiaowei Zhao.

composed of super-capacitor and traditional power supply has been used in many fields [12], such as power battery compensation of electric vehicles [13], train kinetic energy recovery and release [14] and active distribution network system [15], which effectively solves the problems of high instantaneous power and large power fluctuation of traditional power supply. The hybrid power supply provides a feasible solution to the problem of power shortage of EPS under the vehicle power supply in heavy-duty vehicles.

The vehicle power supply is a stable voltage source, while the super-capacitor is a nonlinear time-varying voltage source [16], so the hybrid power supply has different characteristics in vehicle power supply mode, hybrid power supply mode and super-capacitor mode respectively. It is necessary to design corresponding local controllers for different power modes, and switch the local controllers as the power mode changes.

The EPS system with hybrid power supply can be regarded as a hybrid system, which includes continuous event in a single mode and discrete event during power mode switching process [17]. The multi-mode switching control theory is commonly used in hybrid system, such as vehicle body height control [18] and suspension damping control [19]. A fuzzy supervisory controller is usually needed to regulate the multi-mode switching process in order to ensure the stability of the hybrid system, which can make the local controllers switch smoothly by adjusting the weighting coefficient dynamically [20]–[22].

This article focuses on the multi-mode switching control strategy of the EPS with hybrid power supply. Firstly, mathematic model of the EPS system is built. Then the power mode recognition is implemented and the finite automata model is constructed. Considering the different characteristics of the hybrid power supply system in different power modes, the local controllers and the fuzzy supervisory controller respectively are designed to improve control performance of the EPS system. Finally, the simulation was carried out to verify the effectiveness of the control strategy.

II. STRUCTURE AND PRINCIPLE OF THE EPS WITH HYBRID POWER SUPPLY

The EPS with hybrid power supply includes steering wheel, torque/angle sensor, circulating ball steering gear, steering motor, turbine worm reduction mechanism, ECU, super-capacitor, DC-DC converter and vehicle power supply, as shown in the FIGURE 1.

The ECU obtains the target current of steering motor by the target current control algorithm according to steering torque, and vehicle speed. The DC-DC converter is controlled to enable the super-capacitor and the vehicle power supply to generate appropriate current to the steering motor in different power supply modes based on the energy management strategy.

When the required power of steering motor is low, the vehicle power supply drives the steering motor separately and charges the super-capacitor when needed. When the required power of steering motor is high, the super-capacitor, along with the vehicle power supply, provides power for the steering motor. When the vehicle power supply breaks down, the super-capacitor provides power for steering motor emergently.

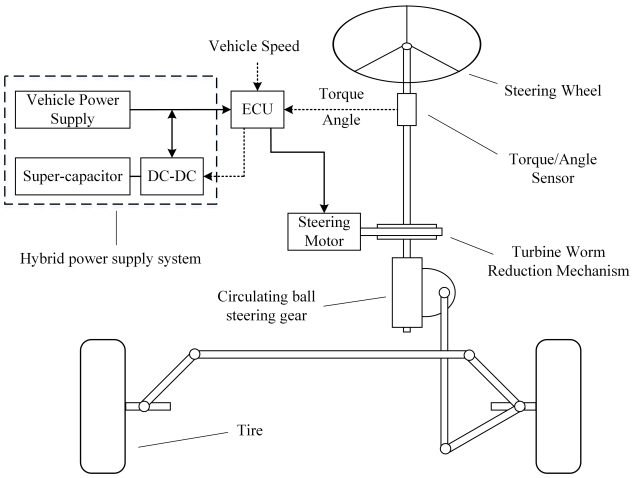

FIGURE 1. Schematic of the EPS with hybrid power supply.

III. MODEL OF THE EPS WITH HYBRID POWER SUPPLY

A. MODEL OF HYBRID POWER SUPPLY SYSTEM

The vehicle power supply is a relatively stable voltage source due to the regulation of voltage regulator in the alternator and the filtration of battery. Therefore, the constant voltage source is chosen as the model of vehicle power supply in this paper.

The super-capacitor is a non-linear time-varying voltage source, and its terminal voltage varies greatly with charging or discharging. A first-order RC model of super-capacitor is constructed in this paper, since it is simple in structure and can accurately reflect the external electrical characteristics of super-capacitor during charging and discharging. The voltage calculation formula of super-capacitor is as follows.

$$U = U_0 - \int i\Delta t \Big/ C \tag{1}$$

where, U_0 is the initial voltage, i is the working current, C is the rated capacitance.

B. MODEL OF EPS

The mathematical model of the circulating ball type EPS is as follow.

$$J_{hw} \cdot \ddot{\theta}_{hw} + B_{hw} \cdot \dot{\theta}_{hw} + K_t(\theta_{hw} - \theta_e) = T_{hw} \tag{2}$$

$$J_m \cdot \ddot{\theta}_m + B_m \cdot \dot{\theta}_m = k_a i - T_a/G \tag{3}$$

$$J_c \cdot \ddot{\theta}_e + B_c \cdot \dot{\theta}_e = K_t(\theta_{hw} - \theta_e) + T_a - PF_L/2\pi \tag{4}$$

$$m_L \cdot \ddot{x}_m + b_L \cdot \dot{x}_m = F_L - F_{cs} \tag{5}$$

$$J_{cs} \cdot \ddot{\theta}_{cs} + B_{cs} \cdot \dot{\theta}_{cs} = F_{cs} \cdot R_{cs} - T_p \tag{6}$$

$$U = L\frac{di}{dt} + Ri + K_e\frac{d\theta_m}{dt} \tag{7}$$

where, $\theta_m = G \cdot \theta_e$, $\theta_e = \frac{2\pi}{P} \cdot x_m$, $x_m = R_{cs} \cdot \theta_{cs}$.

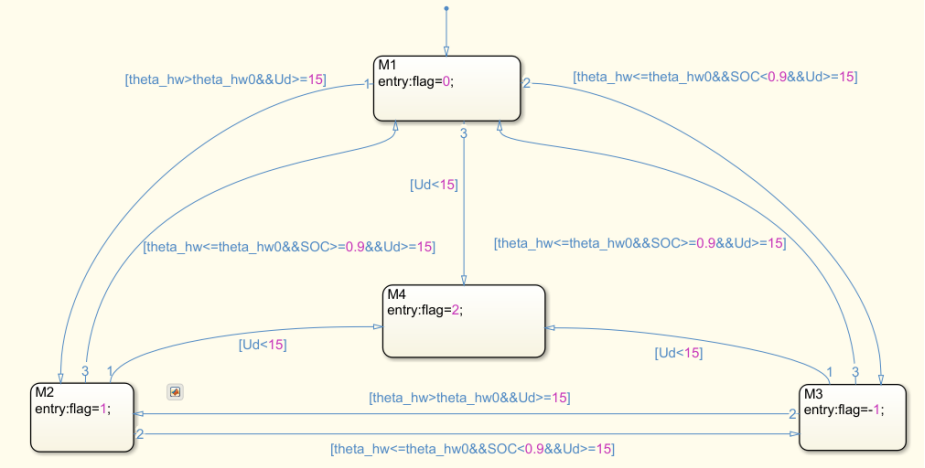

FIGURE 2. Finite automaton model of hybrid power supply system.

Where, J_{hw} is rotational inertia of steering wheel, B_{hw} is damping coefficient of steering wheel, K_t is stiffness coefficient of torsion bar, θ_{hw} is rotational angle of steering wheel, θ_e is rotational angle of screw, T_{hw} is driver input torque, J_m is rotational inertia of steering motor, B_m is damping coefficient of steering motor, θ_m is rotational angle of steering motor, k_a is torque coefficient of steering motor, i is current of steering motor, T_a is assisting torque, G is transmission ratio of turbine worm mechanism, J_c is rotational inertia of screw, B_c is damping coefficient of screw, P is pitch of screw, F_L is thrust force of screw, m_l is mass of nut, b_l is damping coefficient of nut, x_m is displacement of nut, F_{cs} is acting force of sector gear, J_{cs} is rotational inertia of sector gear, B_{cs} is damping coefficient of sector gear, θ_{cs} is rotational angle of sector gear, R_{cs} is radius of pitch circle of sector gear, T_p is steering resistance torque, U is voltage of steering motor, L is inductance of steering motor, R is resistance of steering motor, k_e is back EMF coefficient.

IV. POWER MODE RECOGNITION OF HYBRID POWER SUPPLY SYSTEM

According to the steering angle, state of charge (SOC) of super-capacitor and voltage of the vehicle power supply, power modes of the hybrid power supply system can be recognized, and the corresponding mode recognition signal flag of each mode are obtained, as shown in the TABLE 1.

It can be considered that the steering resistance torque depends on vehicle speed and steering angle. When the steering resistance torque is above the certain threshold in critical state, the vehicle power supply cannot provide enough power for the steering motor, thus the power mode switches to the hybrid power supply mode.

Considering the maximum power which the vehicle power supply can provide to the steering motor, the maximum assistant torque of the steering motor is equal to the certain threshold of steering resistance torque.

TABLE 1. Power modes of hybrid power supply system.

Power modes	State of super-capacitor	Conditions	flag
Vehicle power supply mode	charging	$\theta_{hw} \le \theta_{hw0}$, $SOC < 0.9$	-1
	N/A	$\theta_{hw} \le \theta_{hw0}$, $SOC \ge 0.9$	0
Hybrid power supply mode	discharging	$\theta_{hw} > \theta_{hw0}$	1
Super-capacitor mode	discharging	$U_d < 15$	2

TABLE 2. Steering angle and vehicle speed in critical state.

v	2.96	4	6	8	10	12	14
θ_{hw0}	0	49.83	114.96	169.11	215.13	252.84	283.15

According to the law of steering resistance torque at low speed [23], the steering angle and vehicle speed in critical state are obtained as shown in the TABLE 2.

The equation of steering angle and vehicle speed in critical state is obtained by piecewise polynomial fitting as follows.

$$\theta_{hw0} = f(v) = \begin{cases} 0, & v < 2.96 \\ -1.227 \cdot v^2 + 45.8 \cdot v - 118.4, & v \ge 2.96 \end{cases} \tag{8}$$

Based on the above analysis of power mode recognition, a finite automaton model of hybrid power supply system is constructed in MATLAB/Stateflow, as shown in FIGURE 2. It can be seen form the figure that the initial default working state of the finite automata model is the working state corresponding to flag = 0, in which the super-capacitor does not work; when the system meets the conditions of a state

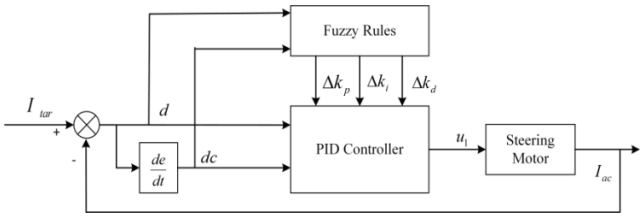

FIGURE 3. Schematic of the fuzzy PID controller.

transition, it will switch to the working state which the state transition points to. The finite automaton model only has one enabled state, and the output value of the model is the flag value corresponding to the enabled state.

V. DESIGN OF MULTI-MODE SWITCHING CONTROLLER

Considering the different electrical characteristics of hybrid power supply in different power modes, the corresponding local controllers are designed, and the fuzzy supervisory controller is designed to ensure the stability of the hybrid system during multi-mode switching process.

A. DESIGN OF LOCAL CONTROLLER

In the vehicle power supply mode, the vehicle usually travels at medium or high speed, which requires higher real-time performance of the steering controller. The fuzzy PID controller can track the target signal quickly for its simple structure compared with other model-based controllers, and its control accuracy is guaranteed for the system [24], [25], thus the fuzzy PID controller is designed as the local controller in this mode.

The fuzzy PID controller is an improved PID controller based on fuzzy rules which are used to realize self-adaptive adjustment of PID parameters. The schematic of the fuzzy PID controller is shown in FIGURE 3.

The fuzzy PID controller is used to conduct the closed-loop control of armature current in steering motor, so as to control the steering assist torque. The input of the PID controller is the difference d between the target current I_{tar} and the actual current I_{ac} of the steering motor. The output of the PID controller is as follows.

$$u_1 = k_p \cdot (I_{tar} - I_{ac}) + k_i \cdot \int (I_{tar} - I_{ac}) + k_d \cdot \left(\dot{I}_{tar} - \dot{I}_{ac}\right) \quad (9)$$

where, k_p is proportional coefficient, k_i is integral coefficient, k_d is differential coefficient.

The inputs of fuzzy rules are the difference d and its change rate dc. For d and dc, the basic domains are both set as [-2, 2], the fuzzy subsets are both {NB, NM, NS, ZO, PS, PM, PB}. For Δk_p, Δk_i and Δk_d, the basic domains are respectively $[-0.008, 0.008]$, $[-0.001, 0.001]$, $[-0.0007, 0.0007]$, the fuzzy subsets are all {NB, NM, NS, ZO, PS, PM, PB}.

In hybrid power supply mode, the interference of the super-capacitor disturbs the voltage of vehicle power supply to a certain extent, which is not conducive to the stable control of the steering system. Active disturbance rejection controller (ADRC) can actively eliminate the effect of voltage disturbance and achieve stable control [26], [27], so the ADRC is designed as the local controller in hybrid power supply mode.

The ADRC consists of tracking differentiator, nonlinear state error feedback law, extended state observer and disturbance compensation. The schematic of ADRC is shown in FIGURE 4.

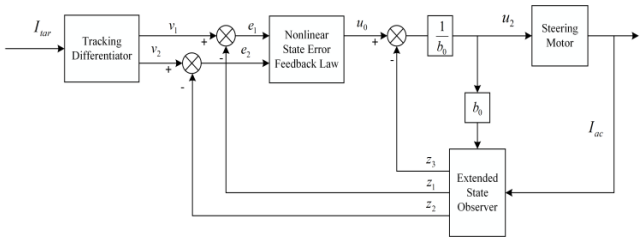

FIGURE 4. Schematic of ADRC.

The inputs of ADRC are the target current and actual current. The output is the control voltage of the steering motor. The formula of each module of ADRC is as follows [28].

Tracking differentiator:

$$\begin{cases} \dot{v}_1 = v_1 + h \cdot v_2 \\ \dot{v}_2 = v_2 + h \cdot fhan\,(v_1 - I_{tar}, v_2, r_0, h) \end{cases} \quad (10)$$

Extended state observer:

$$\begin{cases} e = z_1 - I_{ac} \\ fe = fal\,(e, 0.5, h) \\ fe_1 = fal\,(e, 0.25, h) \\ \dot{z}_1 = z_1 + h \cdot (z_2 - \beta_{01} \cdot e) \\ \dot{z}_2 = z_2 + h \cdot (z_3 - \beta_{02} \cdot fe + b_0 \cdot u) \\ \dot{z}_3 = z_3 + h \cdot (-\beta_{03} \cdot fe_1) \end{cases} \quad (11)$$

Nonlinear state error feedback:

$$\begin{cases} e_1 = v_1 - z_1 \\ e_2 = v_2 - z_2 \\ u_0 = -fhan\,(e_1, c \cdot e_2, r, h_1) \end{cases} \quad (12)$$

Disturbance compensation:

$$u_2 = (u_0 - z_3)/b_0 \quad (13)$$

where:

$$fal\,(x, \alpha, d) = \begin{cases} x/d^{1-\alpha}, & |x| \le d \\ |x|^{\alpha} \cdot sgn\,(x), & |x| > d \end{cases} \quad (14)$$

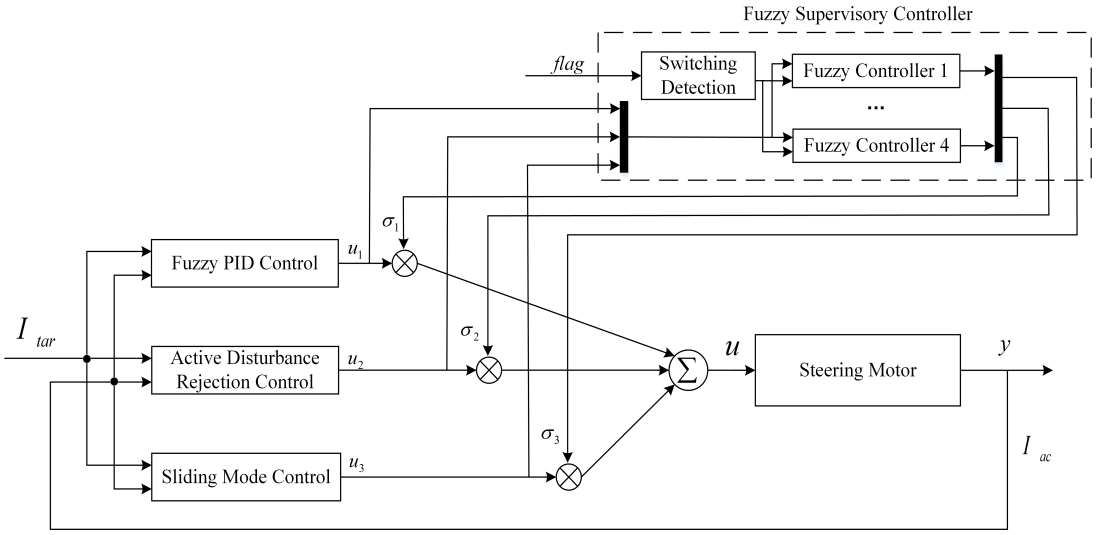

FIGURE 5. Schematic of fuzzy supervisory controller.

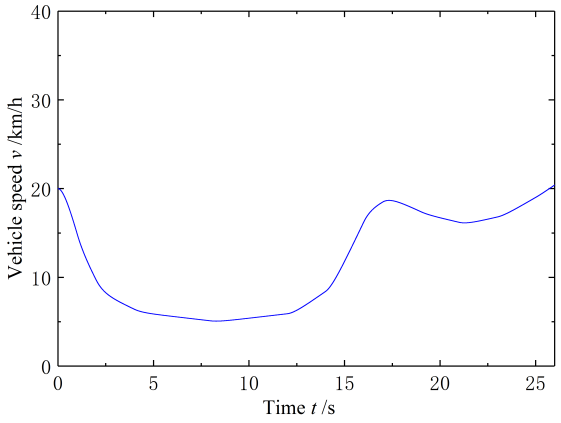

FIGURE 6. Vehicle speed.

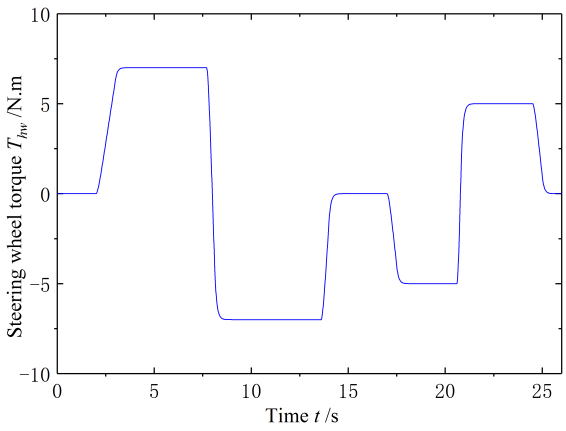

FIGURE 7. Driver input torque.

$$
\begin{aligned}
&fhan\left(x_1, x_2, r, h\right) \\
&= \begin{cases}
d = r \cdot h^2 \\
a_0 = h \cdot x_2 \\
y = x_1 + a_0 \\
a_1 = \sqrt{d \cdot (d + 8 \cdot |y|)} \\
a_2 = a_0 + sign\left(y\right) \cdot \left(a_1 - d\right)/2 \\
s_y = \left(sign\left(y + d\right) - sign\left(y - d\right)\right)/2 \\
a = \left(a_0 + y - a_2\right) \cdot s_y + a_2 \\
s_a = \left(sign\left(a + d\right) - sign\left(a - d\right)\right)/2 \\
fhan = -r \cdot \left(a/d - sign\left(a\right)\right) \cdot s_a - r \cdot sign\left(a\right)
\end{cases}
\end{aligned} \tag{15}
$$

where, h is integration step size, r_0 is velocity factor, β_{01}, β_{02} and β_{03} are system adjustment parameters, r is control gain, c is damping coefficient, h_1 is precision factor, b_0 is compensation factor.

The values of parameters in ADRC are as follows:

$h = 0.01$, $r_0 = 3.5$, $\beta_{01} = 100$, $\beta_{02} = 300$, $\beta_{03} = 1000$, $r = 6$, $c = 2$, $h_1 = 0.02$, $b_0 = 2$.

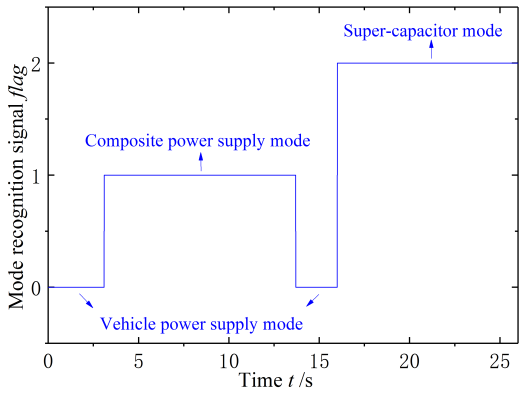

FIGURE 8. The mode recognition signal.

In super-capacitor mode, the super-capacitor provides power to steering motor separately in which discharging process appears nonlinearity. The sliding mode control is a

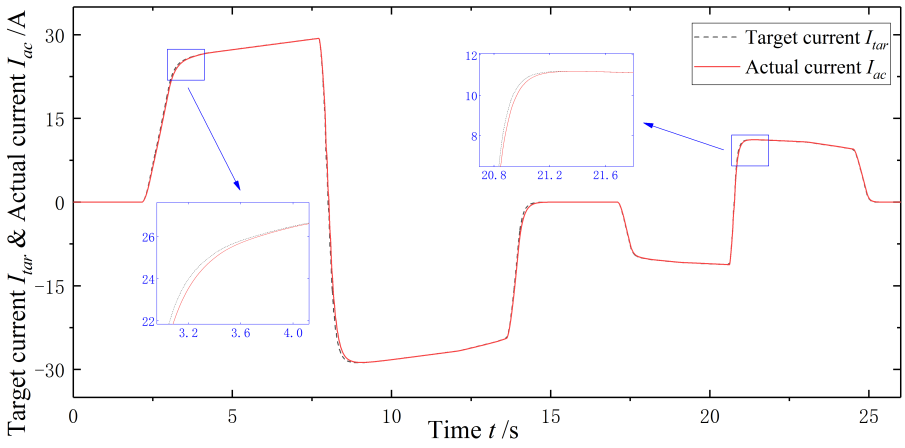

FIGURE 9. The tracking curve of current in steering motor.

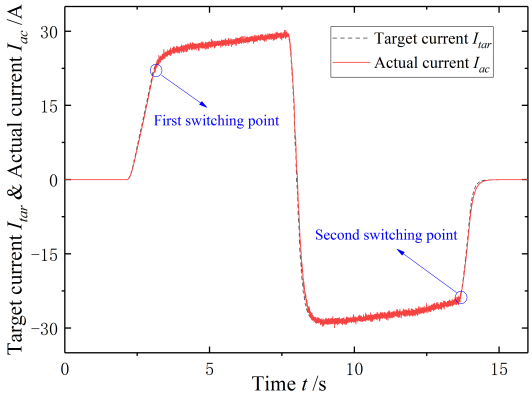

FIGURE 10. Current tracking curve of steering motor.

typical nonlinear control method, so it is selected as local controller in this mode [29], [30].

The difference between the target current I_{tar} and the actual current I_{ac} is selected as sliding surface [31].

$$s = I_{tar} - I_{ac} \tag{16}$$

The derivation of switching surface can be expressed by the following formula.

$$\dot{s} = \dot{I}_{tar} - \dot{I}_{ac} \tag{17}$$

Combining formula 7 and 17, the following formula can be obtained.

$$\dot{s} = \dot{I}_{tar} + \frac{R}{L} \cdot I_{ac} + \frac{k_v}{L} \cdot \dot{\theta}_m - \frac{u_3}{L} \tag{18}$$

The formula of control quantity can be presented as follows by transforming the above formula.

$$u_3 = L \cdot \dot{I}_{tar} + R \cdot I_{ac} + k_v \cdot \dot{\theta}_m - L \cdot \dot{s} \tag{19}$$

The exponential approach law of sliding surface is chosen as follows.

$$\dot{s} = -\varepsilon \cdot sgn\,(s) - k \cdot s \quad (\varepsilon > 0, k > 0) \tag{20}$$

The parameter ε is used to make system reach the sliding surface with a certain speed. The parameter k ensures the realization of sliding mode.

By substituting the exponential approach law into formula 19, the final control quantity of the system can be obtained.

$$u_3 = L \cdot \dot{I}_{tar} + R \cdot I_{ac} + k_v \cdot \dot{\theta}_m + L \cdot \left[\varepsilon \cdot \mathrm{sgn}\,(s) + k \cdot s\right] \tag{21}$$

The values of parameters in sliding mode controller are as follows.

$$\varepsilon = 5, \quad k = 50.$$

B. DESIGN OF FUZZY SUPERVISORY CONTROLLER

In order to ensure the stability of EPS system with hybrid power supply during multi-mode switching process, the fuzzy supervisory controller based on fuzzy rules is designed, in which the output can be obtained by weighting the outputs of local controllers, as shown in the FIGURE 5.

The final output of the controller is obtained by the following formula.

$$u = \sigma_1 \cdot u_1 + \sigma_2 \cdot u_2 + \sigma_3 \cdot u_3 \tag{22}$$

where, u_1, u_2 and u_3 are respectively the output of each local controller. σ_1, σ_2 and σ_3 are respectively the weighting coefficient of each local controller.

According to the last mode recognition signal *flag* and current mode recognition signal *flag'*, the switching signal *sign* which represents the different switching process of local controllers can be obtained. By detecting the switching signal *sign* and controlling the corresponding fuzzy controller, the fuzzy supervisory controller generates two weighting coefficients to realize the switching process from the last local controller to the current local controller. The switching rules of multi-mode switching controller are shown in TABLE 3.

The inputs of fuzzy controller are the difference e between the original output and the weighted output of the target local controller and the change rate ec of the difference.

$$e = u_i - \sigma_i \cdot u_i \quad (i = 1, 2, 3) \tag{23}$$

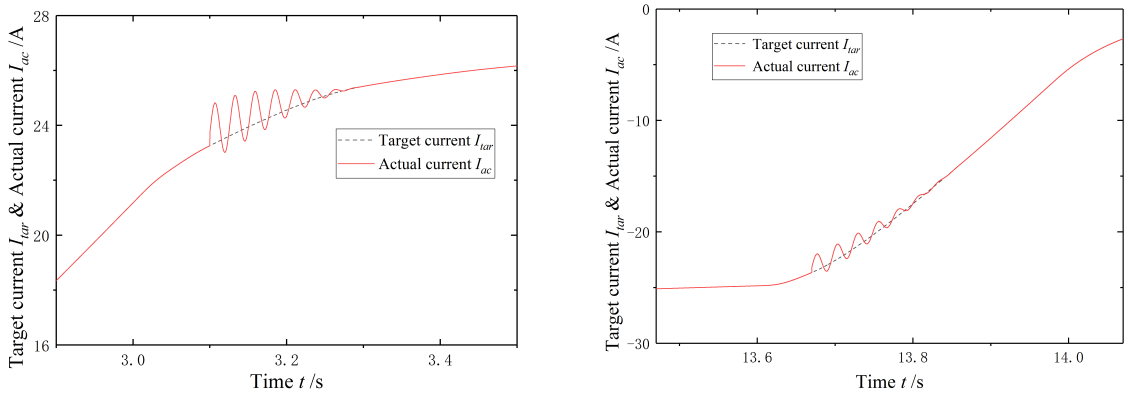

(a) Working current near first switching point

(b)Working current near second switching point

FIGURE 11. Tracking current without fuzzy supervisory controller.

TABLE 3. Switching rules of multi-mode switching controller.

Last mode recognition signal *flag*	Current mode recognition signal *flag'*	Switching signal *sign*	coefficient
-1 or 0	1	1	$\sigma_1 \rightarrow \sigma_2$
1	-1 or 0	2	$\sigma_2 \rightarrow \sigma_1$
-1 or 0	2	3	$\sigma_1 \rightarrow \sigma_3$
1	2	4	$\sigma_2 \rightarrow \sigma_3$

TABLE 4. The fuzzy rules of last weighting coefficients.

ec	*e*					
	ZO	PS1	PS2	PM1	PM2	PB
ZO	ZO	PS1	PS2	PM1	PM2	PB
NM1	ZO	PS1	PS1	PS2	PM1	PB
NM2	ZO	ZO	PS1	PS2	PM1	PM2
NM3	ZO	ZO	PS1	PS1	PS2	PM2
NB	ZO	ZO	ZO	PS1	PS2	PM1

TABLE 5. The fuzzy rules of current weighting coefficients.

ec	*e*					
	ZO	PS1	PS2	PM1	PM2	PB
ZO	PB	PM1	PM1	PS2	PS1	ZO
NM1	PB	PM2	PM2	PM1	PS2	ZO
NM2	PB	PB	PM2	PM1	PS2	PS1
NM3	PB	PB	PM2	PM2	PM1	PS1
NB	PB	PB	PB	PM2	PM1	PS2

For the difference e, the basic domain is set as [0, 24], the fuzzy domain is {0, 0.2, 0.4, 0.6, 0.8, 1}, the fuzzy subset is {ZO, PS1, PS2, PM1, PM2, PB}.

For the change rate ec, the basic domain is set as [−100, 0], the fuzzy domain is {−100, −75, −50, -25, 0}, the fuzzy subset is {ZO, NM1, NM2, NM3, PB}.

For the two weighting coefficients of controller output, the basic domains are both set as [0, 1], the fuzzy domains are both {0, 0.2, 0.4, 0.6, 0.8, 1}, the fuzzy subsets are both {ZO, PS1, PS2, PM1, PM2, PB}.

The fuzzy rules of last weighting coefficient and current weighting coefficient are respectively shown in TABLE 4 and TABLE 5.

VI. VERIFICATION OF THE CONTROL STRATEGY

In order to verify the control strategy of multi-mode switching for the EPS with hybrid power supply, a set of typical working conditions were set up and the simulation was carried out.

A. SETTING OF WORKING CONDITIONS

The working conditions are as follows: The vehicle passes the right-angle bend at low speed, and then turns into a small angle bend when the vehicle power supply breaks down.

Vehicle speed v and driver input torque T_{hw} in the working conditions are shown in FIGURE 6 and FIGURE 7 respectively.

B. ANALYSIS OF SIMULATION RESULTS

The mode recognition signal *flag* in the working conditions are shown in FIGURE 8. It can be seen from FIGURE 8 that the steering system works in vehicle power supply mode at the beginning, and then switches to a hybrid power supply mode because of the increase of steering resistance torque in the right-angle bend. As the steering resistance torque decreases when the vehicle is driving out of the bend, the

system switches back to vehicle power supply mode. After the vehicle has driven out of the bend, the vehicle power supply breaks down and the system switches to super-capacitor mode.

The tracking curve of current in steering motor is obtained as shown in the FIGURE 9. It can be seen from FIGURE 9 that the maximum amplitude of current difference is 0.42A and the lag time of current tracking is only 0.03s in the whole working process, which shows the local controller tracks the target signal rapidly and accurately in different power modes of the hybrid power supply system. The fuzzy supervisory controller effectively ensures the stability of steering system because there is almost no current fluctuation during the switching process.

C. CONTRAST VERIFICATION

Supposed that the local controller still employs the fuzzy-PID controller after the system switches to the hybrid power supply mode, the tracking curve of current in steering motor during the right-angle bend is obtained as shown in the FIGURE 10.

It shows in FIGURE 10 that the fuzzy PID controller cannot eliminate the current fluctuation of steering motor when the power mode switches to hybrid power supply mode, the amplitude of current fluctuation is up to 0.58A. The advantage of ADRC compared with fuzzy PID controller is reflected.

In order to verify the performance of the fuzzy supervisory controller, the simulation of multi-mode switching control without fuzzy supervisory controller is carried out. The results of simulation are shown in FIGURE 11.

It can be seen from the FIGURE 11 that there is current fluctuation of the steering motor with the maximum amplitude of 0.81A at the first switching point, which sustains about 0.22 seconds. At the second switching point, there is current fluctuation of the steering motor with the maximum amplitude of 0.87A, which sustains about 0.19 seconds. The results show that the large fluctuation of current in steering motor advents without fuzzy supervisory controller, which is not conducive to the control stability of steering system and further affect the vehicle handling stability. The superiority of fuzzy supervisory controller is validated by comparing with FIGURE 9.

VII. CONCLUSION

The EPS system with hybrid power supply is constructed to solve the problem that the vehicle power supply of the heavy-duty vehicles cannot provide enough energy for EPS system. The multi-mode switching control strategy is studied. Based on the investigated results, the following conclusions can be drawn.

(1) The mode recognition method is proposed which can accurately identify and switch the power modes of the hybrid power supply system, thus the hybrid power supply system can provide appropriate energy for the steering motor in any cases.

(2) In different power modes of the hybrid power system, the local controllers show excellent performance in tracking target signal, which improves the response speed and control accuracy of steering system.

(3) The fuzzy supervisor make the local controller switch quickly and ensure the stability of steering system during switching process of power modes.

REFERENCES

[1] H. A. Jeyed and A. Ghaffari, "Modeling and performance evaluation of a heavy-duty vehicle based on the hydraulic power steering system," *Simulation*, vol. 95, no. 8, pp. 1–15, Aug. 2019, doi: 10.1177/0037549719866503.

[2] A. Dellamico and P. Krus, "Modeling, simulation, and experimental investigation of an electrohydraulic closed–center power steering system," *IEEE/ASME Trans. Mechatronics*, vol. 20, no. 5, pp. 2452–2462, Oct. 2015, doi: 10.1109/tmech.2014.2384005.

[3] Y. Chen, C. Lü, and J. Xia, "Energy consumption analysis of electro-hydraulic power steering system based on hardware-in-loop simulation test," *Trans. Chin. Soc. Agricult. Eng.*, vol. 26, no. 8, pp. 117–122, Aug. 2018, doi: 10.3969/j.issn.1002-6819.2010.08.020.

[4] L. Xia and H. Jiang, "An electronically controlled hydraulic power steering system for heavy vehicles," *Adv. Mech. Eng.*, vol. 8, no. 11, Nov. 2016, Art. no. 168781401667956, doi: 10.1177/1687814016679566.

[5] B. Tang, H.-B. Jiang, Z. Xu, G.-Q. Geng, and X. Xu, "Dynamics of electromagnetic slip coupling for hydraulic power steering application and its energy-saving characteristics," *J. Central South Univ.*, vol. 22, no. 5, pp. 1994–2000, May 2015, doi: 10.1007/s11771-015-2720-6.

[6] D. Lee, K.-S. Kim, and S. Kim, "Controller design of an electric power steering system," *IEEE Trans. Control Syst. Technol.*, vol. 26, no. 2, pp. 748–755, Mar. 2018, doi: 10.1109/tcst.2017.2679062.

[7] C. Dannöhl, S. Müller, and H. Ulbrich, "H_∞-control of a rack-assisted electric power steering system," *Vehicle Syst. Dyn.*, vol. 50, no. 4, pp. 527–544, Apr. 2012, doi: 10.1080/00423114.2011.603051.

[8] R. A. Hanifah, S. F. Toha, M. K. Hassan, and S. Ahmad, "Power reduction optimization with swarm based technique in electric power assist steering system," *Energy*, vol. 102, pp. 444–452, May 2016, doi: 10.1016/j.energy.2016.02.050.

[9] K. Svancara, J. Priddy, T. Lovric, J. D. Miller, M. Kudanowski, and W. J. Forbes, "Advantages of the alternative method for random hardware failures quantitative evaluation—A practical survey for EPS," *SAE Int. J. Passeng. Cars-Electron. Electr. Syst.*, vol. 6, no. 2, pp. 377–388, Apr. 2013, doi: 10.4271/2013-01-0190.

[10] R. Teymourfar, B. Asaei, H. Iman-Eini, and R. Nejati Fard, "Stationary super-capacitor energy storage system to save regenerative braking energy in a metro line," *Energy Convers. Manage.*, vol. 56, pp. 206–214, Apr. 2012, doi: 10.1016/j.enconman.2011.11.019.

[11] M. Farhadi and O. A. Mohammed, "Event–based protection scheme for a multiterminal hybrid DC power System," *IEEE Trans. Smart Grid*, vol. 6, no. 4, pp. 1658–1669, Jul. 2015, doi: 10.1109/tsg.2015.2396995.

[12] Y. Xiu, L. Cheng, and L. Chunyan, "Research on hybrid energy storage system of super-capacitor and battery optimal allocation," *J. Int. Council Electr. Eng.*, vol. 4, no. 4, pp. 341–347, Oct. 2014, doi: 10.1080/22348972.2014.11011894.

[13] J. Feng, Z. Liu, and M. Zhou, "Research on the energy management of composite energy storage system in electric vehicles," *Int. J. Electr. Hybrid Vehicles*, vol. 10, no. 1, p. 41, 2018, doi: 10.1504/ijehv.2018.10014136.

[14] M. Fallah, M. Asadi, H. Moghbeli, and G. R. Dehnavi, "Energy management and control system of DC–DC converter with super-capacitor and battery for recovering of train kinetic energy," *J. Renew. Sustain. Energy*, vol. 10, no. 1, Jan. 2018, Art. no. 014104, doi: 10.1063/1.5004619.

[15] N. Yan, B. Zhang, W. Li, and S. Ma, "Hybrid energy storage capacity allocation method for active distribution network considering demand side response," *IEEE Trans. Appl. Supercond.*, vol. 29, no. 2, pp. 1–4, Mar. 2019, doi: 10.1109/tasc.2018.2889860.

[16] W. Zuo, R. Li, C. Zhou, Y. Li, J. Xia, and J. Liu, "Battery–supercapacitor hybrid devices: Recent progress and future prospects," *Adv. Sci.*, vol. 4, no. 7, Jul. 2017, Art. no. 1600539, doi: 10.1002/advs.201600539.

[17] O. Diene, M. V. Moreira, E. A. Silva, V. R. Alvarez, and C. F. Nascimento, "Diagnosability of hybrid systems," *IEEE Trans. Contr. Syst. Technol.*, vol. 27, no. 1, pp. 386–393, Jan. 2019, doi: 10.1109/tcst.2017.2757456.

[18] X. Sun, Y. Cai, L. Chen, Y. Liu, and S. Wang, "Vehicle height and posture control of the electronic air suspension system using the hybrid system approach," *Vehicle Syst. Dyn.*, vol. 54, no. 3, pp. 328–352, Mar. 2016, doi: 10.1080/00423114.2015.1136425.

[19] X. Sun, Y. Cai, C. Yuan, L. Chen, and R. Wang, "Hybrid model predictive control of damping multi-mode switching damper for vehicle suspensions," *J. Vibroeng.*, vol. 19, no. 4, pp. 2910–2930, Jun. 2017, doi: 10.21595/jve.2016.17284.

[20] W. Chakchouk, C. Ben Regaya, A. Zaafouri, and A. Sellami, "Fuzzy supervisor approach design based–switching controller for pumping station: Experimental validation," *Math. Problems Eng.*, vol. 2017, pp. 1–12, Nov. 2017, doi: 10.1155/2017/3597346.

[21] C. Bhattacharjee and B. K. Roy, "Fuzzy-supervisory control of a hybrid system to improve contractual grid support with fuzzy proportional-derivative and integral control for power quality improvement," *IET Gener., Transmiss. Distrib.*, vol. 12, no. 7, pp. 1455–1465, Oct. 2017, doi: 10.1049/iet-gtd.2017.0708.

[22] N. Ebrahimi and A. Gharaveisi, "Optimal fuzzy supervisor controller for an active suspension system," *Int. J. Soft Comput. Eng.*, vol. 2, no. 4, pp. 36–39, Sep. 2012.

[23] D. Cao, B. Tang, H. Jiang, C. Yin, D. Zhang, and Y. Huang, "Study on low–speed steering resistance torque of vehicles considering friction between tire and pavement," *Appl. Sci.*, vol. 9, no. 5, p. 1015, Mar. 2019, doi: 10.3390/app9051015.

[24] H. H. Choi, H. M. Yun, and Y. Kim, "Implementation of evolutionary fuzzy PID speed controller for PM synchronous motor," *IEEE Trans. Ind. Inf.*, vol. 11, no. 2, pp. 540–547, Apr. 2015, doi: 10.1109/tii.2013.2284561.

[25] N. N. Sari, H. Jahanshahi, and M. Fakoor, "Adaptive fuzzy PID control strategy for spacecraft attitude control," *Int. J. Fuzzy Syst.*, vol. 21, no. 3, pp. 769–781, Apr. 2019, doi: 10.1007/s40815-018-0576-2.

[26] B. Ahi and A. Nobakhti, "Hardware implementation of an ADRC controller on a gimbal mechanism," *IEEE Trans. Control Syst. Technol.*, vol. 26, no. 6, pp. 2268–2275, Nov. 2018, doi: 10.1109/tcst.2017.2746059.

[27] L. Castañeda, A. Luviano-Juárez, G. Ochoa-Ortega, and I. Chairez, "Tracking control of uncertain time delay systems: An ADRC approach," *Control Eng. Pract.*, vol. 78, pp. 97–104, Sep. 2018, doi: 10.1016/j.conengprac.2018.06.015.

[28] Q. Dong, Y. Liu, Y. Zhang, S. Gao, and T. Chen, "Improved ADRC with ILC control of a CCD–based tracking loop for fast steering mirror system," *IEEE Photon. J.*, vol. 10, no. 4, pp. 1–14, Aug. 2018, doi: 10.1109/jphot.2018.2846287.

[29] Z. Zhou and K. Wang, "Sliding mode controller design for wood drying process," *Wood Sci. Technol.*, vol. 52, no. 4, pp. 1039–1048, Jul. 2018, doi: 10.1007/s00226-018-1006-1.

[30] S. Guo, X. Lin-Shi, B. Allard, Y. Gao, and Y. Ruan, "Digital sliding–mode controller for high–frequency DC/DC SMPS," *IEEE Trans. Power Electron.*, vol. 25, no. 5, pp. 1120–1123, May 2010, doi: 10.1109/tpel.2009.2039356.

[31] V. Utkin, "Discussion aspects of high–order sliding mode control," *IEEE Trans. Autom. Control*, vol. 61, no. 3, pp. 829–833, Mar. 2016, doi: 10.1109/tac.2015.2450571.

BIN TANG received the B.S. degree in electronics and information engineering and the M.S. and Ph.D. degrees in vehicle engineering from Jiangsu University, Zhenjiang, China, in 2007, 2011, and 2015, respectively.

He is currently an Associate Professor with the Automotive Engineering Research Institute, Jiangsu University. His research interests include vehicle system dynamics and control, intelligent steering, and drive control.

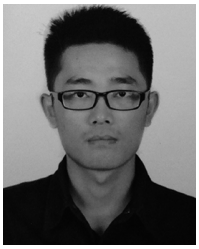

YINGQIU HUANG received the B.S. degree in vehicle engineering from Jiangsu University, Zhenjiang, China, in 2017, where he is currently pursuing the master's degree in vehicle engineering with the School of Automotive and Traffic Engineering.

DI ZHANG received the B.S. degree in automobile service engineering from the Qilu University of Technology, Jinan, China, in 2017.

She is currently pursuing the master's degree in vehicle engineering with the School of Automotive and Traffic Engineering, Jiangsu University, Zhenjiang, China.

HAOBIN JIANG received the B.S. degree from Nanjing Agricultural University, Nanjing, China, in 1991, and the M.S. and Ph.D. degrees from Jiangsu University, Zhenjiang, China, in 1994 and 2000, respectively, all in mechanical engineering.

He is currently a Professor with the Automotive Engineering Research Institute, Jiangsu University. His research interests include vehicle dynamics performance analysis and electronic control technologies for vehicles.